830-H-15 NAS1.60:1561

MAY 2 9

NASA
Technical Paper 1561

AVRADCOM
Technical Report 79-28

COMPLETED

Preliminary Study of Methods for Providing Thermal Shock Resistance to Plasma-Sprayed Ceramic Gas-Path Seals

ORIGINAL

Robert C. Bill, Donald W. Wisander,
and David E. Brewe

MAY 1980

NASA

US ARMY AVRADCOM

24

NASA
Technical Paper 1561

AVRADCOM
Technical Report 79-28

Preliminary Study of Methods for Providing Thermal Shock Resistance to Plasma-Sprayed Ceramic Gas-Path Seals

Robert C. Bill
Propulsion Laboratory, AVRADCOM Research and Technology Laboratories
Lewis Research Center, Cleveland, Ohio

Donald W. Wisander
Lewis Research Center, Cleveland, Ohio

David E. Brewe
Propulsion Laboratory, AVRADCOM Research and Technology Laboratories
Lewis Research Center, Cleveland, Ohio

National Aeronautics
and Space Administration

**Scientific and Technical
Information Office**

1980

Summary

The cyclic thermal shock resistance of several plasma-sprayed-ceramic, turbine-gas-path seal systems was evaluated. The thermal shock cycle consisted of heating the ceramic surface to 1300° to 1350° C for 3½ minutes while the metallic backing to which the ceramic was bonded was maintained at about 500° to 600° C. After the 3½-minute heating portion of the cycle, the ceramic surface was quickly cooled to about 300° C. The cycle was repeated until the ceramic spalled or until 1000 cycles was reached.

Two broad categories of systems were evaluated: those with stepwise-graded-composition, plasma-sprayed metal-ceramic layers between the ceramic (yttria-stabilized ZrO_2) layer and the metalic substrate; and those with a porous-metal, low-modulus pad between the ceramic layer and the metal substrate. The most promising systems were those that had a porous-metal, low-modulus pad as a strain isolator between the ceramic layer and the dense metal substrate. The optimum low-modulus-pad configuration represents a balance between sufficient strength and oxidation resistance for survival on the one hand and sufficient resilience for strain isolation on the other hand. The optimum configuration was not identified. Cooling pins extending into the low-modulus pad significantly reduced the oxidation rate of the porous metal and extended the seal life. The thermal shock resistance of the ceramic layer was improved by increasing its porosity and by precracking it before thermal shock testing. Microstructural and probe studies suggested that the long-term durability of the high-pressure-turbine seal systems would be adversely affected if the metal-ceramic interfaces exceeded about 800° C because some metallic species would rapidly diffuse.

Introduction

The efficiency and performance of a gas turbine engine are very sensitive to gas-path seal clearances throughout the engine. In most cases, the single most significant gas-path seal is the high-pressure-turbine outer air seal, shown schematically in figure 1 (ref. 1). Studies have indicated that, depending on the turbine design, from 1 to 3 percent turbine efficiency loss is suffered for each 1 percent increase in the ratio of blade tip clearance to blade span (ref. 2).

State-of-the-art turbine seal technology is based on the use of metallic seal systems. Three problems are associated with metallic systems: They are prone to gradual clearance degradation due to erosive and corrosive mechanisms at turbine operating temperatures. They are generally nonabradable, so that rubs result in blade tip wear; and this further aggravates the blade tip clearance problem. Furthermore, they require significant amounts of cooling air to maintain them at allowable temperatures, and engine efficiency penalties are associated with the expenditure of this cooling air.

Ceramic materials are an alternative to the currently used metallic systems and hold promise for significantly higher allowable temperatures and improved chemical stability. To perform as an effective high-pressure-turbine seal material, though, the ceramic must afford some degree of abradability and erosion resistance and must be able to survive thermal stresses imposed by the engine operating cycle.

Various ceramic high-pressure-turbine seals are being explored. Systems based on hot-pressed silicon carbide (SiC) and Si-SiC composites (ref. 3), ceramic honeycombs (ref. 4), sintered zirconium dioxide (ZrO_2) (ref. 5), and plasma-sprayed ZrO_2 (ref. 6) have been assessed. Presently, the greatest activity is concentrated on systems incorporating plasma-sprayed, yttria-stabilized ZrO_2; and the most significant concern is to develop methods for providing resistance to cracking and spalling caused by thermal stresses and prolonged exposure to high temperatures.

There are basically two methods of reducing or minimizing the thermal stresses to which the plasma-sprayed ZrO_2 seal system is subjected in the engine environment. These methods are shown schematically in figure 2. One is to grade the material properties in a stepwise or continuous manner by grading the material composition from fully metallic adjacent to the substrate to fully ceramic adjacent to the gas path. This method is summarized in reference 6. The other method is to incorporate a low-density, sintered metal pad or cushion between the ceramic layer and the metallic substrate, as described by Erickson (ref. 7).

Applying a thin NiCrAlY bond coat developed by Stecura (ref. 8) to the system with the low-modulus pad gave this system particularly good resistance to thermal shock failure (ref. 9).

This report evaluates the cyclic thermal shock resistance of several experimental variations of these two methods for reducing thermal stresses. The ultimate goal was to demonstrate survival of 1000 thermal shock cycles. The thermal shock test cycle employed was designed to simulate the range of transient and steady-state conditions imposed during engine operation. One thousand cycles was selected as the goal because after 1000 test cycles the total accumulated time at temperature (50 hr) is significant from the standpoint of diffusion-, creep-, and oxidation-related processes and because 1000 cycles is significant with respect to engine service.

Finite-element thermal stress analyses were also conducted on selected seal designs to determine the significance of various deliberate modifications to material properties. Also, modes of thermal shock failure were identified, and effects of high temperature on the materials' microstructures were studied. Methods of addressing the identified failure modes are suggested.

Apparatus and Procedure

The cyclic thermal shock apparatus is shown in figure 3(a). The specimen was heated with an oxygen-acetylene torch, with the flame impinging directly onto the ceramic surfaces at a 90° angle. While the ceramic surface was being heated, cooling airflow was directed onto the metallic backing. The flame was positioned and tuned so that, during heatup, the ceramic surface reached a stable temperature of about 1315° C within 1 minute for all seal configurations. Heatup lasted 3½ minutes. Cooling airflow to the metallic backing was controlled to 2.4×10^{-3} m^3/sec (5 ft^3/min) for all specimens, with associated backing temperatures of 480° to 540° C, depending on specimen configuration. Ceramic surface temperatures were monitored by an infrared pyrometer and were cross-checked by Chromel-Alumel thermocouples embedded in a few special calibration specimens. Temperatures at other locations in the seal and on the metallic backing were measured by Chromel-Alumel thermocouples in all specimens.

After the specimen was held in the flame for 3½ minutes, the pneumatic actuator moved it into the cooldown position. During cooldown, which lasted for 1 minute, a cooling airflow of 1.2×10^{-3} m^3/sec (2.5 ft^3/min) was directed onto the ceramic surface; $2.41 \times 10^{-3} m^3$/sec (5 ft^3/min) of cooling air continued to flow over the metallic backing. The ceramic surface was thereby cooled from its maximum of 1315° C to about 450° C in several seconds. By the end of cooldown the entire specimen was at about 300° C. The cycle was then repeated. A representative time-temperature schedule for the entire thermal cycle is shown in figure 3(b). Temperatures are indicated for the ceramic surface and the metallic backing.

Materials

Two methods for providing a thermal-shock-resistant seal system based on plasma-sprayed ZrO_2 were evaluated in this study and are shown in figure 2. The first method was to incorporate intermediate layers of plasma-sprayed metal-ceramic composites between the dense metallic substrate and the ceramic layer adjacent to the gas path. The metal-ceramic intermediate layers would mitigate thermal stresses imposed on the ZrO_2 by gradually varying the thermal expansion and mechanical properties from those of the metallic substrate to those of the ceramic layer. The second method was to incorporate a low-modulus strain isolator pad of porous metal between the dense metallic substrate and the ceramic layer. The isolator pad allows the ceramic layer and the metallic backing to undergo thermal expansion and contraction independently.

One series of ceramic layers was made of nonprealloyed ZrO_2-Y_2O_3 powders (i.e., a mechanical mixture of ZrO_2 and Y_2O_3 powders). The remaining ceramic layers were prepared from prestabilized ZrO_2 – 12-wt% Y_2O_3 powder, –200 + 325 mesh size (and are henceforth referred to as "YSZ"). Standard spray conditions (for the Plasmadyne SG-1 gun) included a 550-ampere arc current, a 10-centimeter standoff distance, and argon as the powder carrier and arc gas. The arc gas flow rate was 4.6×10^{-4} m^3/sec (60 ft^3/hr), and the powder gas flow rate was 9.3×10^{-5} m^3/sec (12 ft^3/hr). The powder feed setting was 3.0. In addition, a series of specimens was prepared under modified spray conditions intended to increase the porosity of the YSZ layer. The standoff distance was 15 to 20 centimeters and the gun current was 500 amperes; other spray conditions were the same as those for the standard YSZ. The ceramic layer thus produced was designated "YSZ (porous)."

In the first method for controlling thermal stresses, two plasma-sprayed, metal-ceramic composite intermediate layers were used (fig. 2). Directly beneath the ZrO_2 layer was a 750-micrometer-thick layer of 80-wt% ZrO_2 – 20-wt% NiCrAlY. In turn, beneath that layer was a

20-wt%ZrO_2–80-wt% NiCrAlY layer, again 750 micrometers thick. Between that layer and the 304-stainless-steel substrate was a NiCrAlY bond coat, about 50 to 75 micrometers thick. Spray parameters used for the 80-wt% YSZ–20-wt% NiCrAlY layer were the same as those used for the standard YSZ layer. The parameters used for the 20-wt% YSZ–80-wt% NiCrAlY layer were the same as those used for the NiCrAlY bond coat: namely, a 350-ampere arc current, a 4.2×10^{-4}-m^3/sec arc gas flow rate (argon), a 9.3×10^{-5}-m^3/sec powder gas flow rate (argon), and a powder feed setting of 23. The forward plasma feed port was used. Composition (in wt%) of the NiCrAlY used was Ni-16Cr-6Al-0.6Y. The known or estimated room-temperature properties of all plasma-sprayed layers are summarized in table I(a).

In the second method for controlling thermal stresses, a porous-metal, low-modulus pad was provided between the ceramic layer and the 304-stainless-steel substrate. Various compositions, densities, and particulate structures were used to obtain a range of properties so that the potential of this method could be explored. The compositions and the known or estimated properties of these pads are summarized in table I(b). In all cases, a 50-micrometer-thick NiCrAlY bond coat was applied to the low-modulus pad before the ceramic layer was added. The plasma-sprayed layers were applied after the low-modulus pad material was brazed to the 304-stainless-steel substrate. In all systems except LM-1, a gold-palladium-nickel (PAL-1) foil braze was used.

Results and Discussion

Fully Plasma-Sprayed Systems

Thermal shock results. — The cyclic thermal shock performance of five variations on the plasma-sprayed seal system with two sprayed ceramic-metal (cermet) intermediate layers is summarized in figure 4. The "baseline" fully sprayed specimens were prepared by using the standard spray parameters and materials described in the section Materials. All variations on the baseline involved modifications to the ceramic layer, with the intermediate-layer composition and structure remaining constant.

The first series of thermal shock tests applied to the baseline (YSZ) samples resulted in early failure of all specimens, usually on the first cycle. It was decided that the first few cycles were extraordinarily severe because there was insufficient time for the 304-stainless-steel substrate to approach the nominal temperature indicated in figure 2. The thermal stresses that resulted from rapidly heating the ceramic surface to the 1315° C steady-state temperature on a cold metallic substrate were significantly higher than those encountered when the 304-stainless-steel substrate was hot. Therefore, the experimental thermal shock procedure was adjusted. In the first five or six cycles, rather slow heating rates were used so that the substrate would gradually approach the end-of-cycle temperatures indicated in figure 2. After these initial "warmup" cycles, the thermal cycles were in accordance with that shown in figure 2. When this modified test procedure was used, the average cyclic life of the baseline specimens was 36 cycles (indicated by the asterisk in fig. 4). The failure sequence consisted of the gradual, easily observed propagation of "mudflat" cracks through the ceramic layer, with final spalling of about one half of the ceramic layer. An example of such a spalled specimen is shown in figure 5. The laminar crack leading to final spalling always began at the interface between the ceramic layer and the first intermediate layer, apparently at a specimen corner.

The low-density modification to the ceramic layer, YSZ (porous), was subjected to the original unmodified test sequence. Failures did not occur in the first thermal shock cycle, as was the case for the baseline specimens; and the average cyclic life was 42 cycles. This improved performance of the specimens incorporating the low-density ceramic layer is believed to have two causes: First, the elastic modulus of the low-density ceramic layer was approximately 25 percent lower than that of the standard ceramic layer, as indicated in table I. A comparative three-dimensional stress analysis, summarized in figure 6, shows that stresses in the ceramic layer are significantly reduced if the modulus of elasticity is reduced. Second, the degree and type of porosity present in a brittle material are known to strongly influence resistance to crack propagation, usually so that crack growth is retarded (refs. 10 and 11). This is discussed in more detail later.

Deliberately introducing a network of "mudflat" cracks into the ceramic layer surface significantly improved cyclic thermal shock resistance, as shown in figure 4. Precracking was achieved by uniformly heating the specimens to 480° C and then quenching the ceramic surface against an ethanol-saturated pad. The crack spacing generated by this treatment was about 6 millimeters, and the cracks penetrated about 30 to 40 micrometers through the YSZ layer. A specimen so treated survived 44 of the original unmodified thermal shock cycles, as compared with less than 1 cycle for the baseline. The precracking is

believed to have provided stress relief to the ceramic layer.

As shown in figure 4, there was little difference between the performance of the baseline specimens and those prepared with nonprealloyed Y_2O_3-ZrO_2 composite powders. In both cases, failure occurred on the first standard thermal shock cycle. When the modified thermal shock test sequence was followed, the specimens prepared with the nonprealloyed powders performed slightly better than the baseline specimens.

Based on the results reported herein, increasing the ceramic porosity and precracking the ceramic layer appear to be effective ways of improving the thermal shock resistance of the fully sprayed systems. There are numerous examples in the literature in which it is demonstrated both analytically and experimentally that the fracture toughness and thermal shock resistance of a brittle material can be improved if certain microcrack or porosity distributions are present (refs. 10 to 12). The morphology of pores in a plasma-sprayed structure is in fact crack-like, with the crack plane lying in the plane of the sprayed layer. Hence, we believe the role of porosity in cyclic crack propagation through the plasma-sprayed ceramic to be like that of a fine microcrack network. As developed by Manning and Lineback (ref. 11) the Griffith energy *GE*, a measure of crack propagation resistance, is given by

$$GE = \gamma\left(\frac{1}{\pi c} + 2Nc\right)$$

where γ is the surface energy of the material, c is the pore size, or microcrack length, and N is the number of cracks per unit of cross-sectional area. The $2Nc$ term in the *GE* expression accounts for the effect of reduced elastic modulus on the strain energy available for crack propagation. From the micrographs shown in figure 7, we concluded that the increased number of pores N, rather than variations in pore size c, improved thermal shock resistance.

These theoretical and analytical considerations suggest interesting approaches to further improving the thermal shock resistance of plasma-sprayed ceramic seal systems. One approach for future consideration might be to increase the number of crack-like pores or microcracks by incorporating fugitive additives into the plasma-sprayed ceramic structure and then either burning or leaching the additives out of the ceramic matrix. Yet another way of increasing thermal shock resistance might be to include controlled amounts of partially stabilized or nonstabilized ZrO_2 in the ceramic layer. The Griffith energy for crack propagation would then be increased either by fracture of the partially stabilized ZrO_2 particles, leading to increased microcrack density, or by transformation toughening of the ceramic material in front of a propagating crack tip. The incorporation of partially stabilized particles in a ceramic matrix was used to good effect by Claussen (ref. 13) in producing a tough sintered Al_2O_3-ZrO_2 ceramic composit.

Microstructural studies. — The effects of exposing the intermediate-layer materials to high temperatures for extended periods of time were studied by scanning electron microscopy and microprobe analyses. The objective was to determine the temperature limitations of the intermediate layers from the standpoint of long-term survival of the seal system.

Optical photomicrographs (figs. 8(a) and (b)) of sections through the cermet layers in the as-sprayed condition and after exposure to 927° C in air for 50 hours show some interesting comparisons. In the as-sprayed condition, the interiors of the NiCrAlY particles were clean and pore free and the interfaces between metal and ceramic particles were quite well defined. After the layers had been exposed to 927° C for 50 hours, fine pores were apparent in the interior of the metallic particles, and the interfaces between the metal and ceramic particles had become broader and had a "fringed" appearance. Higher magnification SEM photcgraphs (fig. 8(c)) verify the interior porosity and show a distinct separate phase filling the interface between the metal and ceramic particles. The average thickness of this "interfacial phase" after 50 hours at 927° C is about 1 micrometer.

The effects of time at temperature on the structure of the cermet layers were further studied by using the elemental mapping capabilities of the microprobe. As shown in figure 9, nickel and chromium were quite uniformly distributed in the NiCrAlY particles in the as-sprayed condition. Aluminum, however, shows evidence of segregation to distinct regions at extremities of the metallic particles. We believe that this segregation in the as-sprayed condition was the result of nonequilibrium cooling of molten metallic particles upon deposition. The ceramic constituent shows some segregation of yttrium in the as-sprayed condition, again probably as a result of nonequilibrium cooling. Yttrium concentration in the NiCrAlY was too low to show significant evidence for or against uniform distribution.

After the cermet layer was exposed to 927° C for 50 hours, elemental distribution was dramatically changed, as indicated in figure 10. Aluminum had

almost completely diffused from the interior of the NiCrAlY particles to the metal-ceramic interfaces, with significant concentration to a depth of 0.5 micrometer into neighboring ceramic particles. Also, the concentration of chromium was visibly higher in the interfacial regions than in the interior of the metallic particles. Areas of higher than average yttrium concentration were present in the ceramic regions, similar to those seen in the as-sprayed microstructure (fig. 8), though such areas do not happen to be shown in figure 9.

Samples that were exposed in air to 760° C for 200 hours and to 982° C for 50 hours are shown in figure 11. The thickness of the interfacial phase after 200 hours at 760° C was difficult to measure, but it was estimated to be about 0.1 micrometer. After 50 hours at 982° C the interface was 1.5 to 2.5 micrometers thick.

The interfacial thickness measurements from several specimens are summarized in table II. The results are fairly consistent with a parabolic growth rate of the interfacial layer and an apparent activation energy of 146 kJ/g mole (35 kcal/g mole) for the growth mechanism. The parabolic rate is consistent with growth controlled by aluminum and chromium diffusion through the interfacial layer, rather than with diffusion through the metallic particle interiors. Compared with published oxide film growth activation energies (ref. 14), however, the activation energies that seem to apply here are quite low. Perhaps the interfacial layer is more highly defective than the oxide films that form on alloy surfaces oxidized in air.

From these microstructural studies we concluded that the porosity observed to develop in the metallic particle interiors was due to extensive diffusion of aluminum and, to a lesser extent, chromium from the interiors to the interfacial regions. Very likely, this is the mechanism responsible for swelling the cermet layers after exposure to high temperatures, as reported in reference 15. Since swelling of the cermet intermediate layers would impose tensile stresses on the ceramic top layer, it is considered detrimental to the long-term survival of the sprayed, graded-layer system.

Therefore, a primary concern and overall limitation of sprayed ceramic seal systems with cermet intermediate layers is that temperatures of the cermet layers be maintained at less than 800° C. Thermal analysis indicates that these layers are exposed to extreme temperatures of 900° to 950° C during thermal shock cycling. This temperature can be reduced by increasing the ceramic layer thickness or by increasing the cooling airflow to the metallic backing.

Low-Modulus-Pad Systems

Thermal shock results. — Cyclic thermal shock test results for the seal systems incorporating porous, low-modulus, metallic intermediate layers between the ceramic and the 304-stainless-steel substrate are summarized in figure 12. Known properties for the low-modulus-intermediate-layer systems are reported in table I. The system with the intermediate layer made of 0.125-micrometer-(0.005-in.-)diameter sintered Hoskins-875 wire served as the baseline and is designated LM-1. The results for the LM-1 system were reported in reference 9 and are briefly summarized herein.

Although the average thermal shock life of the LM-1 specimens with the NiCrAlY bond coat was 364 cycles, the longest life of all the configurations tested, mudflat cracking was observed rather early, after 20 to 30 cycles. Interestingly, LM-1 specimens prepared without the bond coat suffered complete loss of the YSZ layer after 20 to 30 cycles. Metallographic sectioning of a specimen that survived 455 cycles without spalling revealed extensive laminar cracking. The laminar cracks apparently began at the interface between the bond coat and the ceramic layer and propagated into the ceramic, as shown in figure 13. From the analytical studies of reference 13, we concluded that performance could be improved if materials with a lower elastic modulus than that of the baseline were used as a low-modulus pad.

Four alternative low-modulus materials were evaluated as strain isolator pads, and their performance is summarized in figure 12. Two of these were low-density, sintered metal-fiber materials: One was a material incorporating sintered equiaxed particles; and one was a low-density, plasma-sprayed NiCrAlY material.

The specimens incorporating a sintered Hastelloy-X pad with a modulus of about 1724 MPa (250 000 psi), designated "LM-2," survived an average of 30 thermal shock cycles before failure. This in itself would hardly seem to indicate the effectiveness of further reducing the modulus of the pads. However, no mudflat cracking of the ceramic occurred and, in fact, the sintered metal itself failed. Thus, there may have been some enhanced strain isolation effectiveness. Details of this failure mechanism are discussed in a later section. In essence though, the Hastelloy-X sintered fiber-metal failed right under the ceramic layer because of excessive temperatures. The temperature at this interface was estimated to have reached 1000° to 1050° C. The appearance of the failure is shown in figure 14.

A material similar to the low-density, sintered Hastelloy-X fiber-metal — but composed of a higher temperature, more oxidation-resistant FeCrAlY fiber — was evaluated as a low-modulus pad material. This system, designated "LM-3," had an average cyclic thermal shock life of 96 cycles. The failure mode was the same as that for LM-2. Excessive temperatures in the sintered fiber-metal led to delamination of the entire ceramic layer, with some heavily oxidized fiber-metal adhering to the delaminated ceramic. Thus, it would appear that, although thermal stresses in the ceramic and at the ceramic-bond coat interface were effectively reduced in both systems LM-2 and LM-3, this benefit was obtained at the cost of reduced life for the intermediate layer itself.

Low density, sintered, equiaxed NiCrAl particles comprised the low-modulus pad used in the LM-4 specimens. The elastic modulus of this material (2.1 GPa) was between that of the baseline (6.09 GPa) and the sintered fiber-metal systems evaluated (1.72 GPa). Cyclic thermal shock testing indicated an average life of 91 cycles. Failure occurred by delamination of the ceramic from the intermediate layer. Laminar cracks that led to spalling were in the ceramic layer or at the interface between the ceramic layer and the bond coat. Also, mudflat cracking was observed after 20 to 30 thermal shock cycles. The failure sequence for LM-4 was quite similar to that of the baseline, LM-1. The reasons why LM-4 specimens did not survive as long as the baseline specimens are not immediately clear. One explanation, though presently unverified, is that the NiCrAl particles of the LM-4 system underwent gradual oxidational swelling and thereby imposed higher stresses to the ceramic layer than were imposed in the baseline configuration.

Finally, cyclic thermal shock tests of the plasma-sprayed, porous NiCrAlY low-modulus system, designated "LM-5," demonstrated an average life of 42 cycles. Failure occurred at the metal-ceramic interface, and mudflat cracks appeared after about 20 cycles. Performance could probably be improved if a thicker porous NiCrAlY layer were employed. Indeed, the low-modulus material used in the LM-4 system was far less effective when its thickness was reduced to the 1.5-millimeter thickness of the sprayed, porous NiCrAlY layer. Applying thicker layers is difficult with the hand-held spray equipment used to make these specimens: Crowning of the sprayed layers makes thickness control, especially near the edges, very difficult. The microstructures of the sprayed, porous layers resulting from both NiCrAlY plasma-spray parameters and polyester plasma-spray parameters are shown in figure 15. The NiCrAlY spray parameters were selected for making the microstructures to be evaluated in seal specimens because they give more uniform porosity distribution than the polyester spray parameters. The structure was about 50 percent porous, and evidently the polyester filler had been completely burned out by the pretest heat treatment.

The seal specimens incorporating low-modulus strain isolator pads showed considerably more thermal shock resistance than specimens with the plasma-sprayed metal-ceramic composite intermediate layers. The performance of the strain isolator pad material could be further improved if elastic moduli considerably lower than that of the LM-1 baseline could be obtained without compromising the durability of the low-modulus pad material. Also, the occurrence of failure associated with the YSZ-NiCrAlY bond-coat interface suggests that performance might be improved by using different bond-coat materials and procedures. Microstructural studies of failure regions in low-modulus-pad specimens provided more detailed insight into failure mechanisms and causes.

Microstructural studies. — Cracks were observed near the interface of the ceramic layer and the NiCrAlY bond coat applied to the Hoskins-875 fiber-metal pad in the baseline low-modulus system, LM-1 (fig. 13). Higher magnification photographs of the crack region and the NiCrAlY bond coat adjacent to the crack (fig. 16) showed internal porosity in the NiCrAlY particles, as was seen in the metal-ceramic layers after exposure to high temperature. Also, energy-dispersive X-ray analysis indicated considerably increased aluminum content near the metal-ceramic layer interface and at the interfaces between adjacent NiCrAlY particles in the bond coat. Though direct supporting evidence is not at hand, these observations do suggest that gradual, progressive laminar crack growth may be enhanced by gradual dimensional changes of the plasma-sprayed constituents and other diffusional effects. As was recommended for the sprayed metal-ceramic intermediate layers, it would appear that long-term survival of the low-modulus-pad concept requires careful control of maximum temperatures at the interface between the ceramic layer and the NiCrAlY bond coat.

A further life-limiting mechanism was seen in the low-modulus systems LM-2 and LM-3. Recall that in these systems laminar failure occurred in the low-modulus layer. Examination of low-modulus material near the laminar failure, where temperatures reached 850° C, revealed that extensive internal porosity had developed in the metalic particles, with some of the sintered bonds

damaged (figs. 17(a) and (b)). Also, a very thick oxide film had formed on the particle surfaces. In comparison, Hastelloy-X particles near the braze bond with the 304-stainless-steel substrate, where temperatures never exceeded 600° C, were nearly free of internal voids and the sinter bonds were quite sound (fig. 17(c)).

We concluded from the microstructural studies that consideration must be given to ways of reducing the maximum temperature in the low-modulus pad and in the bond coat beneath the YSZ layer. Besides increasing the YSZ layer thickness or increasing cooling airflow to the backing, this temperature reduction can be affected by increasing the thermal conductivity through the low-modulus pad. One way of increasing thermal conductivity through the pad is to provide cooling pins integral with the 304-stainless-steel backing and extending almost all the way through the low-modulus pad. This method and its effectiveness are described in the next section.

Effectiveness of cooling pins. — An analytical study performed in reference 16 indicated that temperatures in the low-modulus intermediate layer could be significantly reduced without increasing stresses on the ceramic layer if there were conduction pins through the intermediate layer. Specially modified 304-stainless-steel backings with machined pins in various arrays, depicted in figure 18, were fabricated to further explore this idea. Low-modulus sintered pads of LM-3 composition were mechanically pressed over the pin array and brazed in place. Three pin arrays, representing different total pin areas, were evaluated in this study. Also evaluated was a low-modulus pad pierced with 50-micrometer- (2-mil-) diameter wires, intended to function as flexible pins and thus increase the conductivity through the low-modulus layer. The results of cyclic thermal shock experiments performed on these systems are summarized in figure 19.

The configuration affording the largest pin area failed, after four cycles, at the interface between the ceramic layer and the NiCrAlY bond coat — hardly an improvement over the 91 cycles survived by the LM-3 system without pins. A possible marginal improvement was observed for the small-pin array (second configuration in fig. 18), and a distinct improvement was observed with the coarse pin array (third configuration in fig. 18). Also, the specimen with the 50-micrometer-diameter wire array performed significantly better than the LM-3 configuration. Though no direct temperature measurements were made in the low-modulus layers themselves, the thermocouple data from the 304-stainless-steel substrates indicated that some increased conductivity through the low-modulus pad was taking place. Cycle temperatures near the interface between the substrate and the low-modulus pad were generally higher for the configurations with pin arrays and wires than for the straight LM-3 configuration.

Conclusions

From the cyclic thermal shock experiments conducted in this study, the following conclusions were drawn:

1. The low-modulus-substrate approaches proved to be more effective methods of reducing thermal stresses in the ceramic layer and preventing spalling than were the sprayed, graded-composition approaches.
2. None of the low-modulus substrate materials evaluated were optimum from the standpoint of having a low enough modulus to minimize thermal stresses yet sufficient strength to resist ultimate failure themselves.
3. For both the sprayed, graded-composition intermediate layer and the low-modulus intermediate layer approaches, microstructural studies revealed that if the temperature of the ceramic NiCrAlY particle interfaces exceeded about 800° C, considerable diffusion and segregation of aluminum and chromium to the interfaces occurred. This is believed to shorten the life of the structure because considerable porosity within the NiCrAlY particles results from this diffusion.
4. Increasing the porosity of the YSZ layer and precracking the layer both effectively improved cyclic thermal shock resistance.
5. Cooling pins extending through the low-modulus layers to the 304-stainless-steel substrate improved the durability of the seal system in cyclic thermal shock testing. This is believed to be due partly to reduced temperatures in the low-modulus material near the YSZ layer interface.

Lewis Research Center,
National Aeronautics and Space Administration,
Cleveland, Ohio, July 26, 1979,
505-04.

References

1. Ludwig, Lawrence P.; and Bill, Robert C.: Gas Path Sealing in Turbine Engines. NASA TM-73890 Revised, 1978.
2. Roelke, Richard J.: Miscellaneous Losses. Turbine Design and Application. Vol. 2. A.J. Glassman, ed., NASA SP-290, 1973, Chapt. 8, pp. 125-148.
3. Schwab, R.C.; and Darolia, R.: Feasibility of SiC Composite Structures for 1370° C Gas Turbine Seal Applications. R77AEG160-10, General Electric Co., 1977.

4. Solomon, N.G.; and Vogan, J.W.: Advanced Ceramic Materials for High Temperature Turbine Tip Seals. (RDR-1831-23, International Harvester Co.; NASA Contract NAS3-20061.) NASA CR-135319, 1978.
5. Schlike, P.W.: Advanced Ceramic Seal Program (Phase I). PWA 6635, Pratt & Whitney Aircraft, 1974. (AD-781004).
6. Bill, R.C.; Shiembob, L.T.; and Stewart, O.L.: Development of Sprayed Ceramic Seal System for Turbine Gas Path Sealing. NASA TM 79022, 1978.
7. Erickson, A.F.; Nablo, J.C.; and Panzera, C.: Bonding Ceramic Materials to Metallic Substrates for High-Temperature Low-Weight Applications. ASME Paper 78-WA/GT-16, Dec. 1978.
8. Stecura, S.: Two Layer Thermal Barrier Coating for High Temperature Components. Am. Ceram. Soc. Bull., vol. 56, no. 12, Dec. 1977, pp. 1082-1085.
9. Bill, Robert C.; and Wisander, Donald W.: Preliminary Study of Cyclic Thermal Shock Resistance of Plasma Sprayed Zirconium Oxide Turbine Outer Air Seal Shrouds. NASA TM-73852, 1977.
10. Hasselman, D.P.H.: Unified Theory of Thermal Shock Fracture Initiation and Crack Propagation in Brittle Ceramics. J. Am. Ceram. Soc., vol. 52, no. 11, 1969, pp. 600-604.
11. Manning, C.R.; and Lineback, L.D.: The Role of Surface Energy in Thermal Shock of Ceramics Materials. International Symposium on Special Topics in Ceramics, Surfaces and Interfaces of Glass and Ceramics, Materials Science Research, Vol. 7, V.D. Frechette, W.C. LaCourse, and V.L. Burdick, eds., Plenum Press, 1974.
12. Bansal, G.K.: Effects of Ceramic Microstructure on Strength and Fracture Surface Energy. Ceramic Microstructures '76, Westview Press, 1976, pp. 860-871.
13. Claussen, Nils: Stress Induced Transformation of Tetragonal ZrO_2 Particles in Ceramic Matrices. J. Am. Ceram. Soc., vol. 61, no. 1-2, Jan.-Feb., 1978, pp. 85-86.
14. Hauffe, K. (K. Vorres, transl.): Oxidation of Metals. Plenum Press, 1965, p. 249.
15. Shiembob, L.T.: Development of a Plasma Sprayed Ceramic Gas Path Seal for High Pressure Turbine Application. (PWA-5569-12, Pratt & Whitney Aircraft Group; NASA Contract NAS3-20623.) NASA CR-135387, 1978.
16. Kennedy, Francis E., Jr.; and Bill, Robert C.: Thermal Stress Analysis of Ceramic Gas Path Seal Components for Aircraft Turbines. NASA TP-1437, 1979.
17. Taylor, Christopher M.; and Bill, Robert C.: Temperature Distributions and Thermal Stresses in a Graded Zirconia/Metal Gas Path Seal System for Aircraft Gas Turbine Engines. NASA TM-73818, 1978.

TABLE I.—PROPERTIES OF MATERIALS

(a) Plasma-sprayed materials

Composition	Modulus of elasticity		Thermal conductivity[a]		Hardness	
	GPa	psi	W/m K	Btu/hr ft °F	R_{15Y}	R_{45Y}
YSZ (std.)	12.5	1.8×10^6	0.79	0.46	88	79
YSZ (porous)	9.5	1.4×10^6	----	----	80	70
80-wt% YSZ - 20-wt% NiCrAlY	16.5	2.4×10^6	[a]1.6	.92	Off scale	
20-wt% YSZ - 80-wt% NiCrAlY	[a]58.6	[a]8.5×10^6	[a]2.25	1.3	Off scale	

(b) Low-modulus-pad systems

Designation	Material or composition, wt%	Density (100 minus % porosity)	Modulus of elasticity		Thermal conductivity,[b] W/m K	Hardness, R_{15Y}
			GPa	psi		
LM-1	Hoskins-875	35	6.09	0.89×10^6	0.8	25
LM-2	Hastelloy-X	21	1.72	$.25 \times 10^6$	.35	-180
LM-3	Fe-20Cr-6Al-0.02Y	21	1.68	$.24 \times 10^6$	.35	-170
LM-4	Ni-15Cr-5Al	30	2.1	$.3 \times 10^6$	----	52
LM-5	Ni-16Cr-6Al-0.6Y	~50	10	1.5×10^6	----	49

[a]Thermal conductivity data and one elastic modulus used in analysis are actually for YSZ/CoCrAlY system from ref. 17.
[b]Data from manufacturers' estimates.

TABLE II. — INTERFACIAL FILM THICKNESS STUDY

Thermal exposure		Measured film thickness, μm	Predicted film thickness,[a] h, μm
Time, t, hr	Temperature, T, K		
50	1255	1.5 - 2.5	2.5
200	1033	0.1 - 0.2	.25
20	1173	0.5 - 1	.60
2	1200	0.3 - 0.6	.27
2	1144	0.3 - 0.5	.13
2	1033	Not resolvable	.025

[a]Prediction based on $h = Ae^{(-Q/RT)}t^{1/2}$, where A = 0.45 $m/(hr)^{1/2}$ and Q = 146 kJ/g mole (35 kcal/g mole).

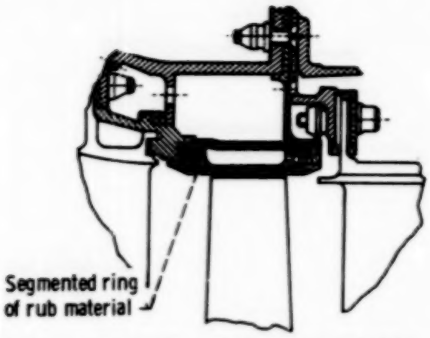

Figure 1. - Schematic of high-pressure-turbine outer air seal.

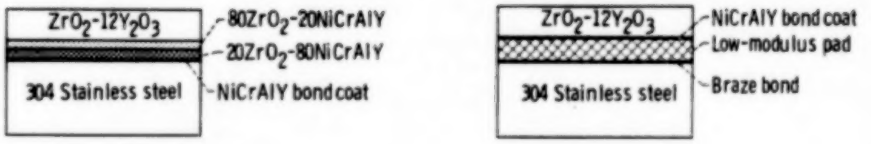

(a) Plasma-sprayed metal-ceramic intermediate layer concept.

(b) Sintered-metal, low-modulus intermediate pad concept.

Figure 2. - Schematic representation of the two turbine seal concepts evaluated. (Compositions are in weight percent.)

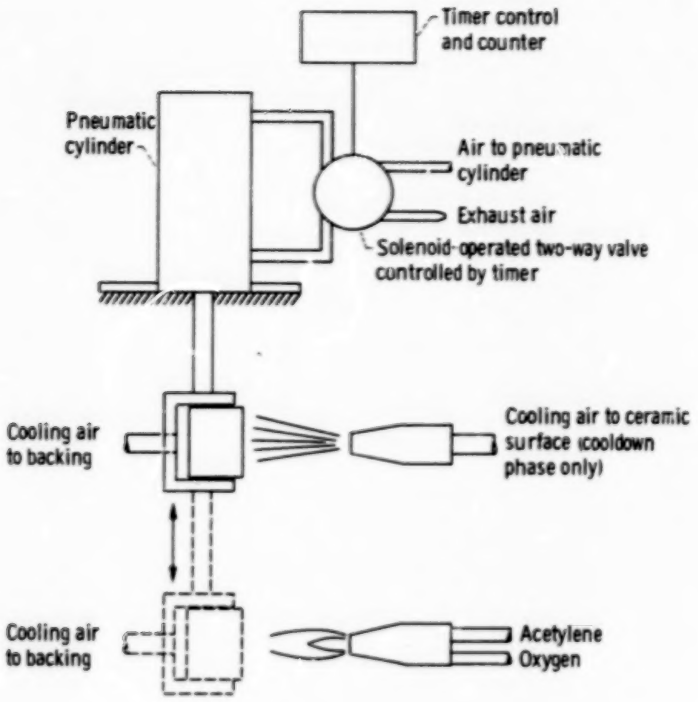

(a) Thermal shock apparatus.

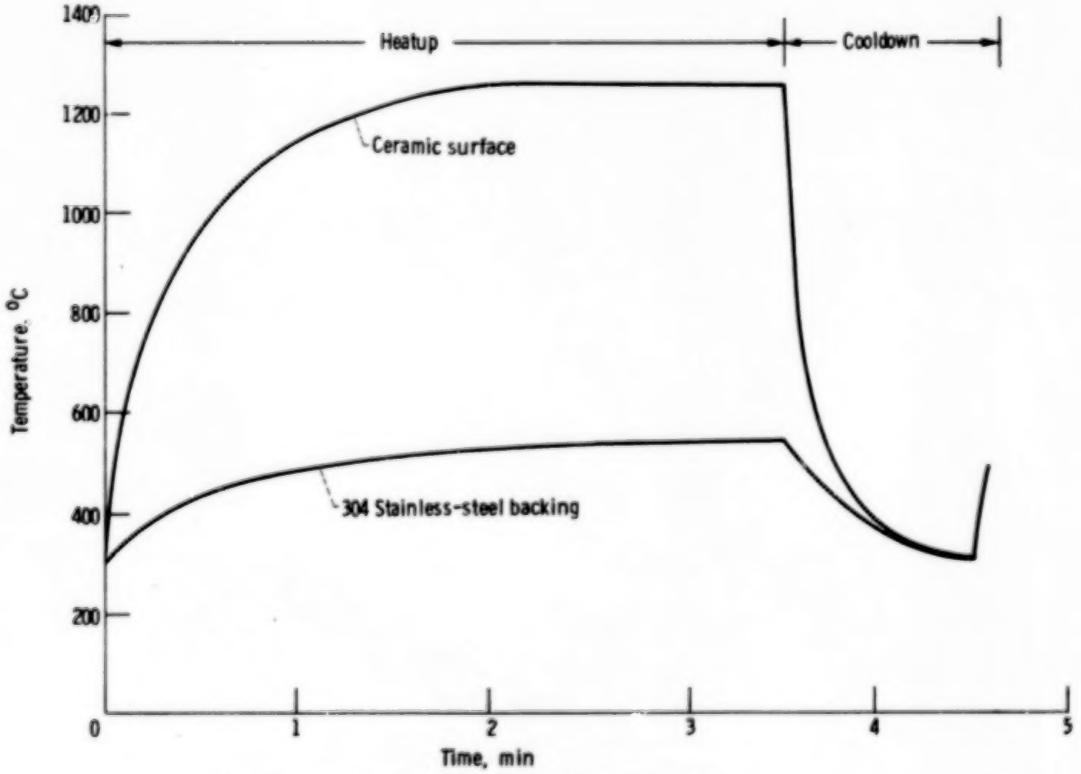

(b) Representative time-temperature plot for thermal shock cycle.

Figure 3. - Thermal-shock rig and test cycle.

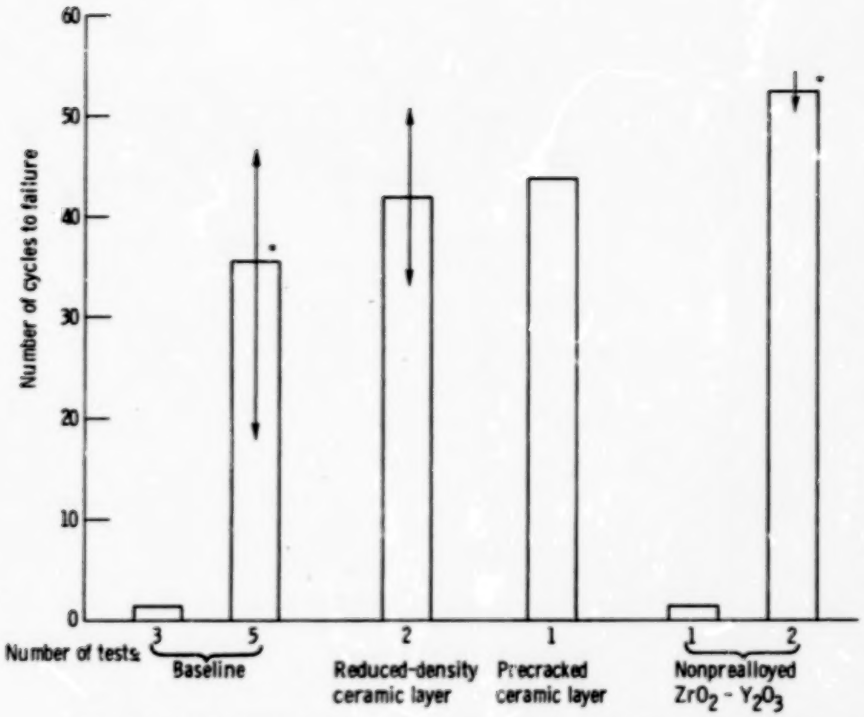

Figure 4. - Cyclic thermal shock lives of plasma-sprayed ceramic seal specimens with sprayed metal-ceramic intermediate layers. (Asterisks denote that first 7 or 8 cycles have been modified.)

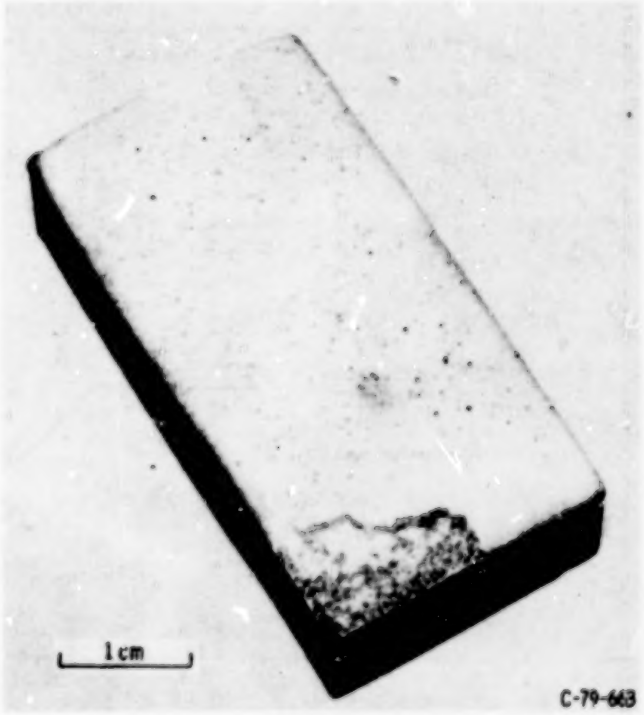

Figure 5. - Baseline fully sprayed specimen, showing spalled coatings after 47 thermal shock cycles.

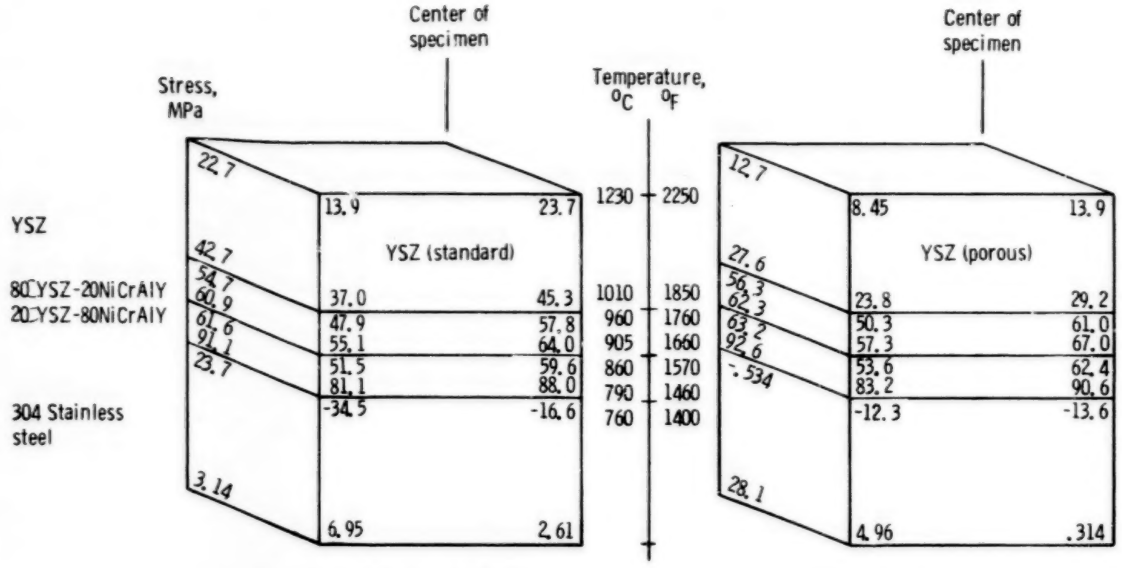

(a) Modulus of elasticity, 12 410 MPa.

(b) Modulus of elasticity, 9660 MPa.

Figure 6. - Effect of YSZ modulus of elasticity on thermal stress distribution through specimen 209 seconds into thermal cycle. (Temperature distribution is also represented. Quarter symmetry element of full specimen is shown. Properties of 80YSZ-20NiCrAlY and 20YSZ-80NiCrAlY layers are those indicated in table I.)

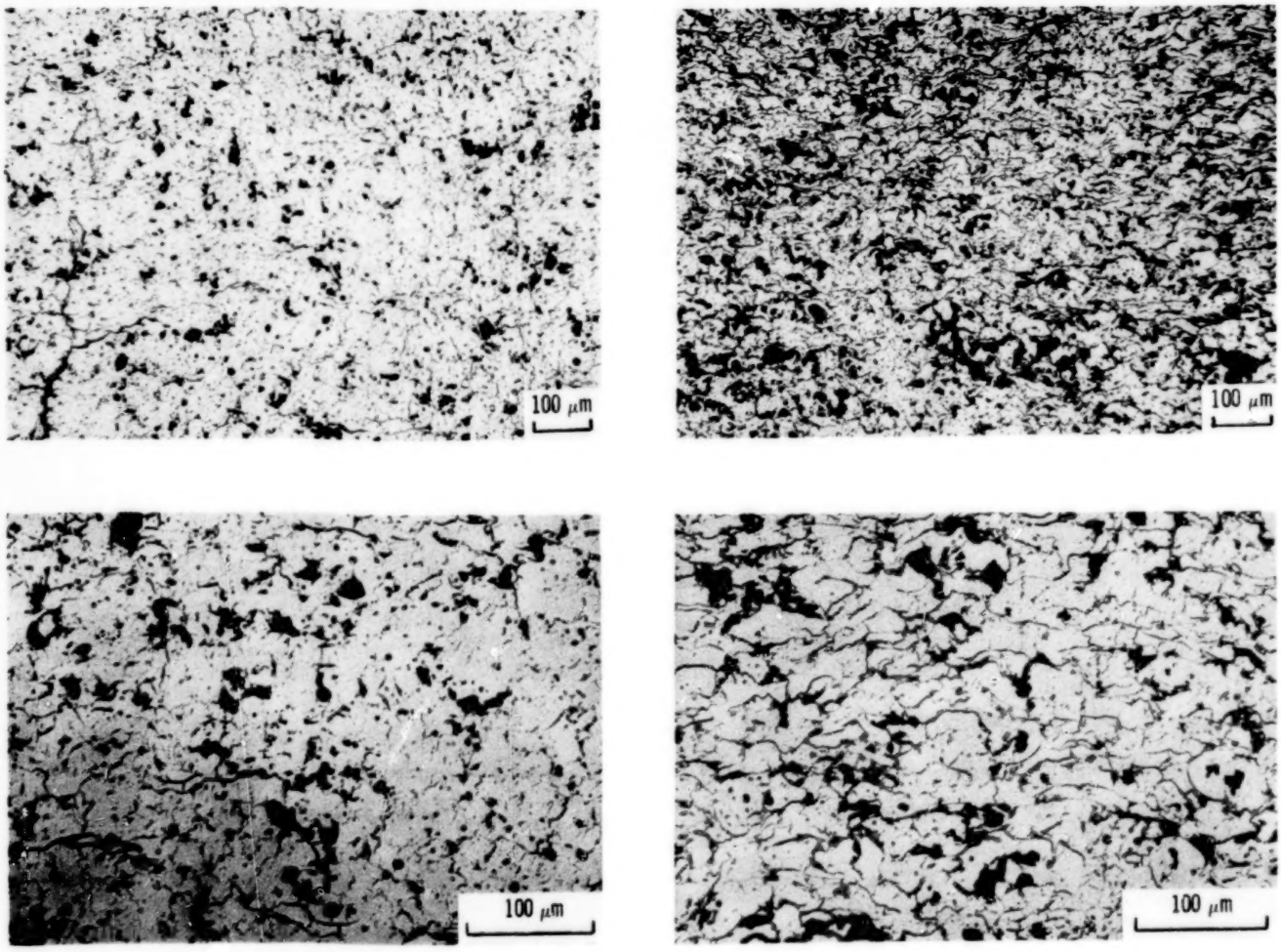

(a) Standard spray conditions (standard YSZ).

(b) Reduced-intensity spray conditions (porous YSZ).

Figure 7. - Microstructures of yttria-stabilized zirconium dioxide prepared under standard and reduced-intensity plasma-spray conditions.

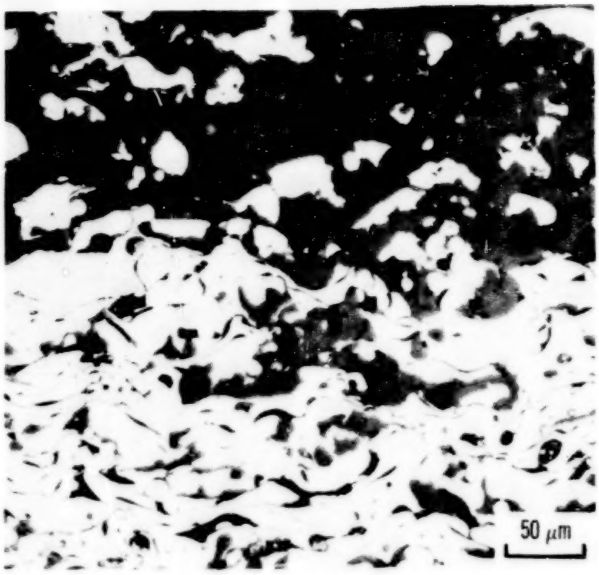

(a) As sprayed; X250.

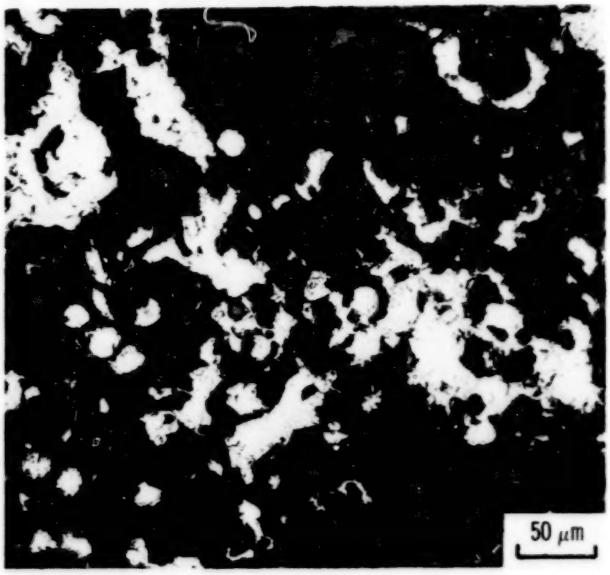

(b) After 50 hours at 927° C; X250.

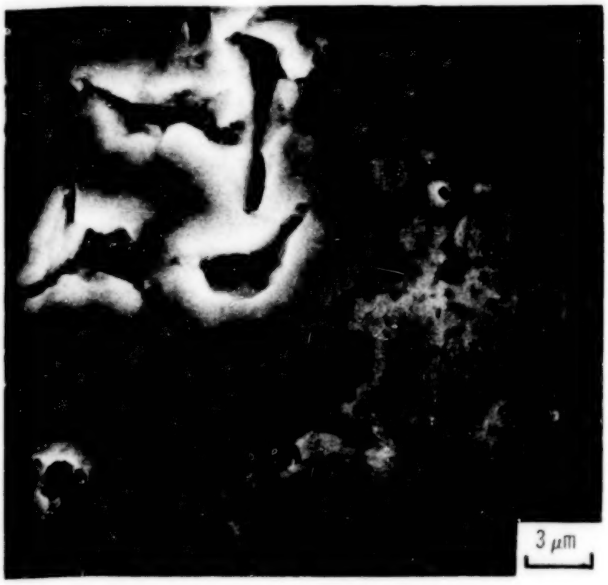

(c) After 50 hours at 927° C; X3000.

Figure 8. - Photomicrographs of YSZ-NiCrAlY layers as sprayed and after exposure at 927° C for 50 hours.

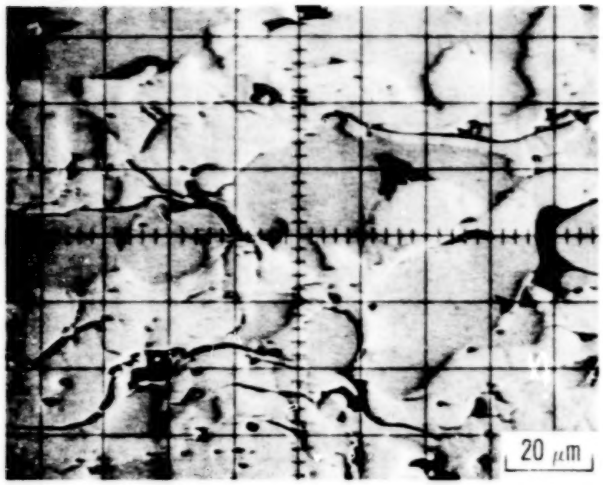

(a) Secondary-electron image.

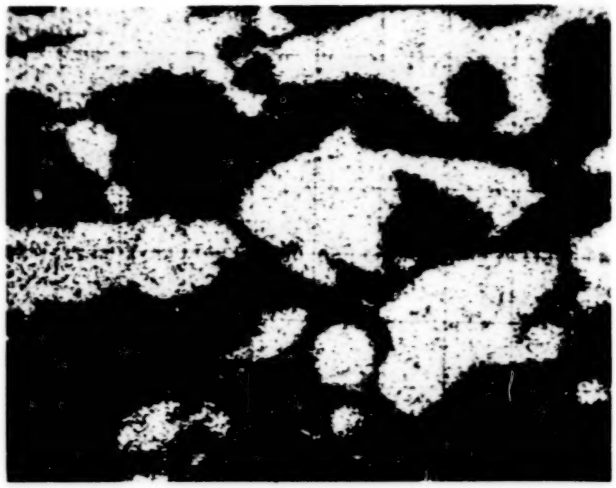

(b) Nickel distribution.

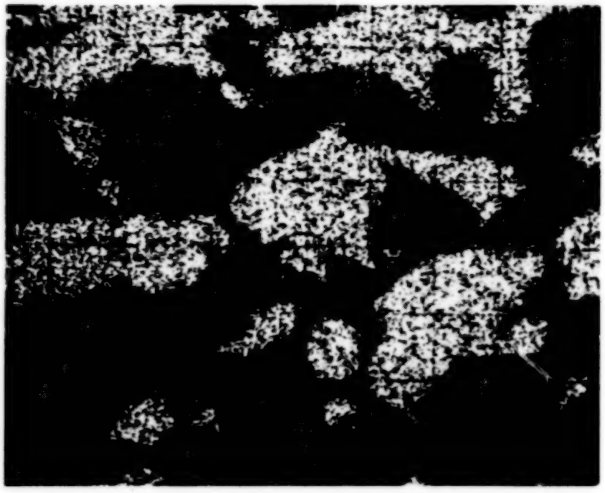

(c) Chromium distribution.

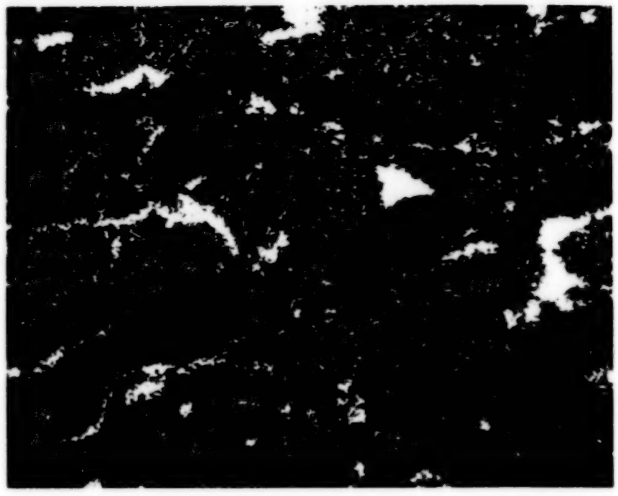

(d) Aluminum distribution.

(e) Zirconium distribution.

(f) Yttrium distribution.

Figure 9. - Elemental distribution of 80YSZ-20NiCrAlY layer in as-sprayed condition.

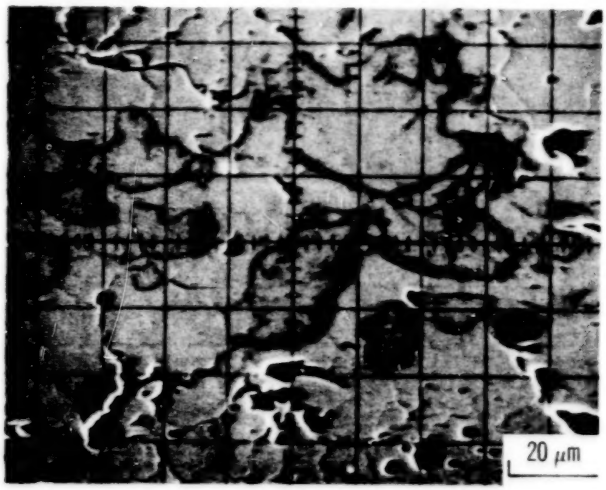

(a) Secondary-electron image.

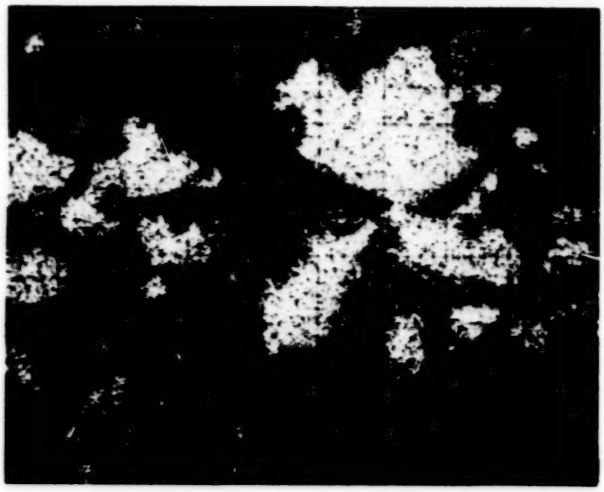

(b) Nickel distribution.

(c) Chromium distribution.

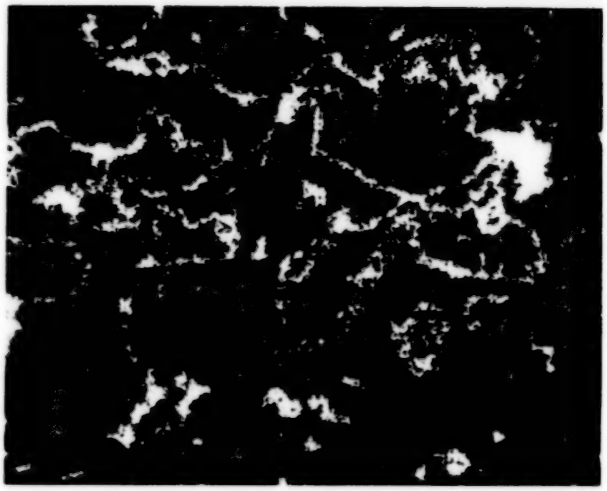

(d) Aluminum distribution.

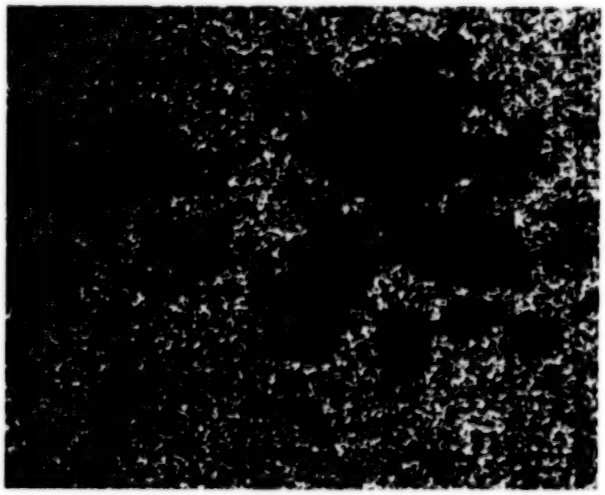

(e) Zirconium distribution.

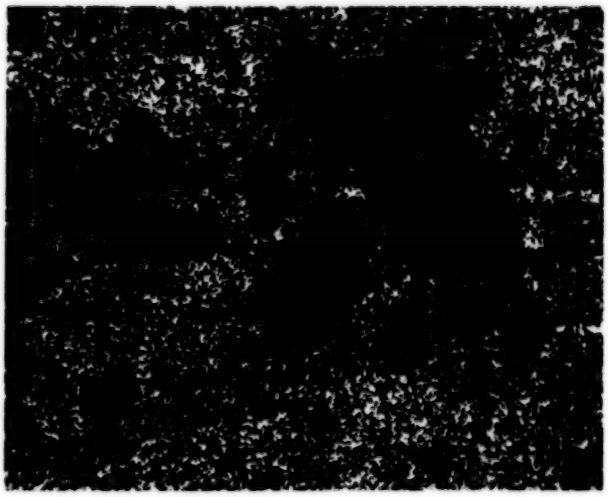

(f) Yttrium distribution.

Figure 10. - Elemental distribution of 80YSZ-20NiCrAlY layer after 50 hours at 927° C.

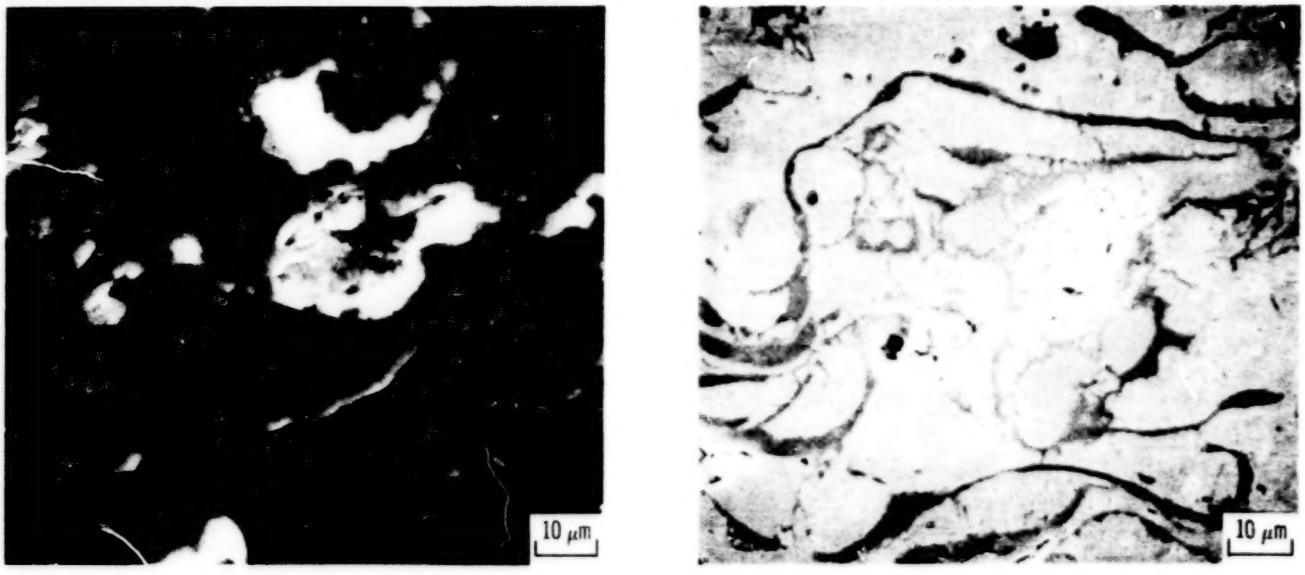

(a) After 200 hours at 760° C.

(b) After 50 hours at 982° C.

Figure 11. - Effect of thermal exposure on microstructure of 20YSZ-80NiCrAlY layers. Of particular interest are thicknesses of interfacial diffusion zones between metallic and ceramic particles.

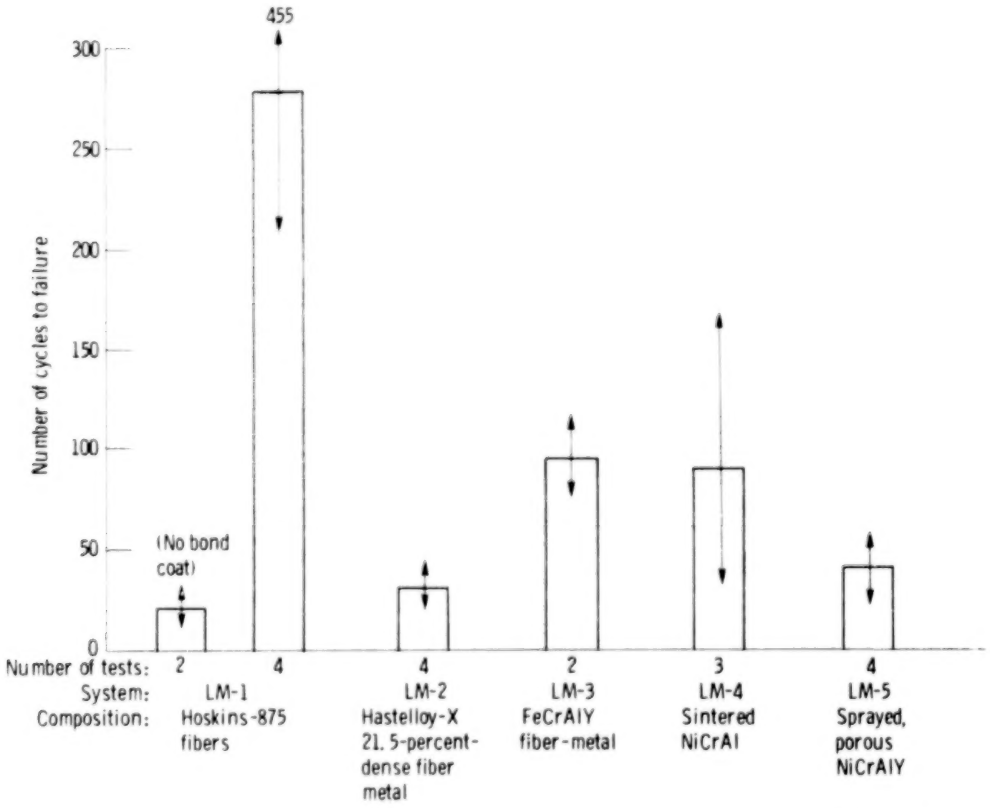

Figure 12. - Cyclic thermal shock lives of plasma-sprayed ceramic zeal specimens with low-modulus pads.

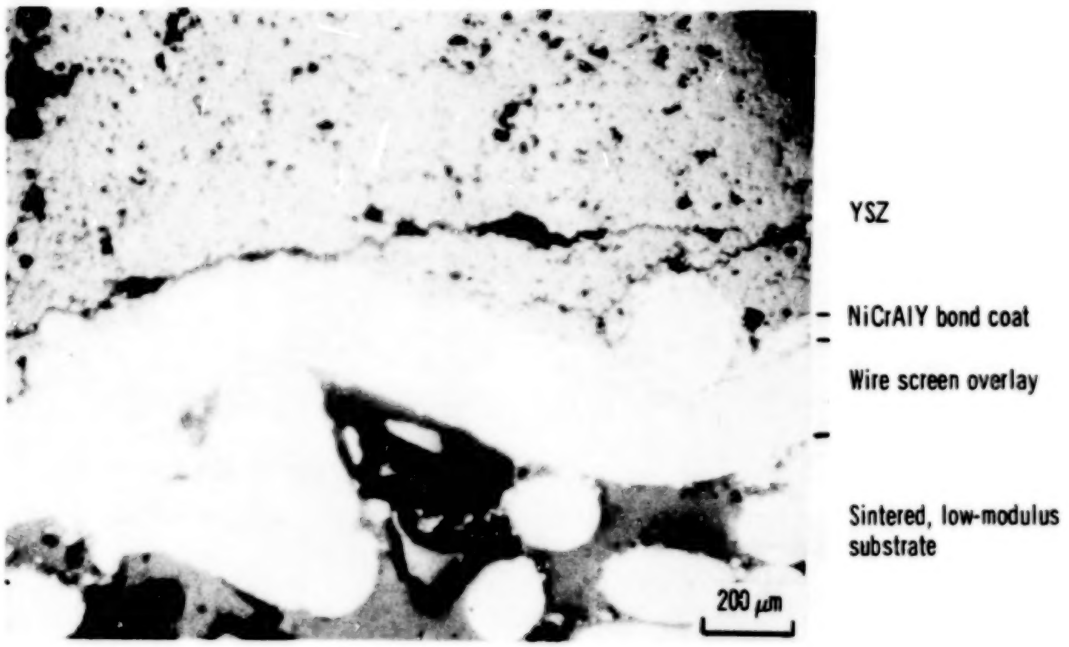

Figure 13. - Microsection through low-modulus-pad system LM-1, showing laminar cracks at and near interface between ceramic and NiCrAlY bond coat. X65.

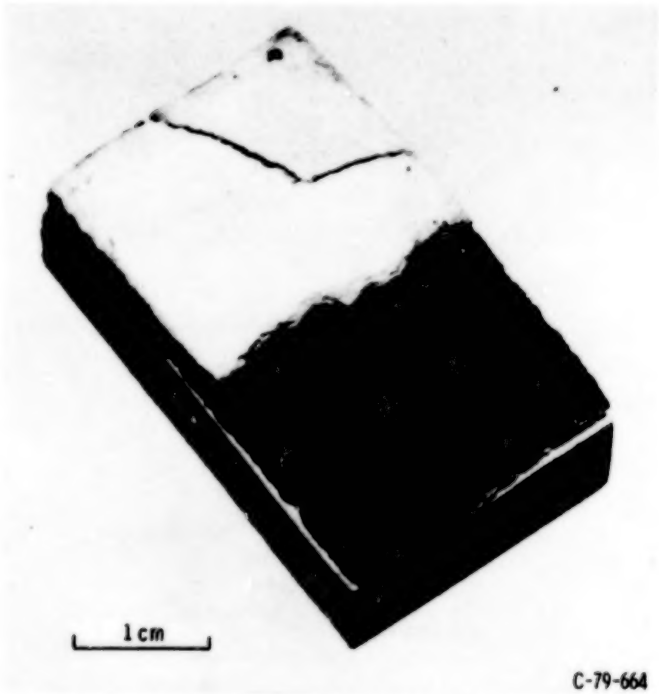

Figure 14. - LM-3 specimen after 79 thermal shock cycles, showing failure in low-modulus material.

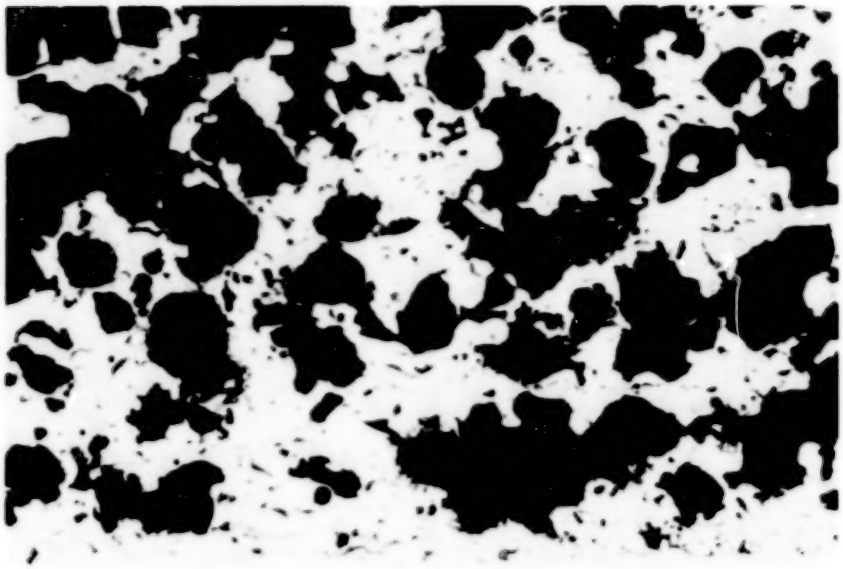

(a) NiCrAlY spray parameters.

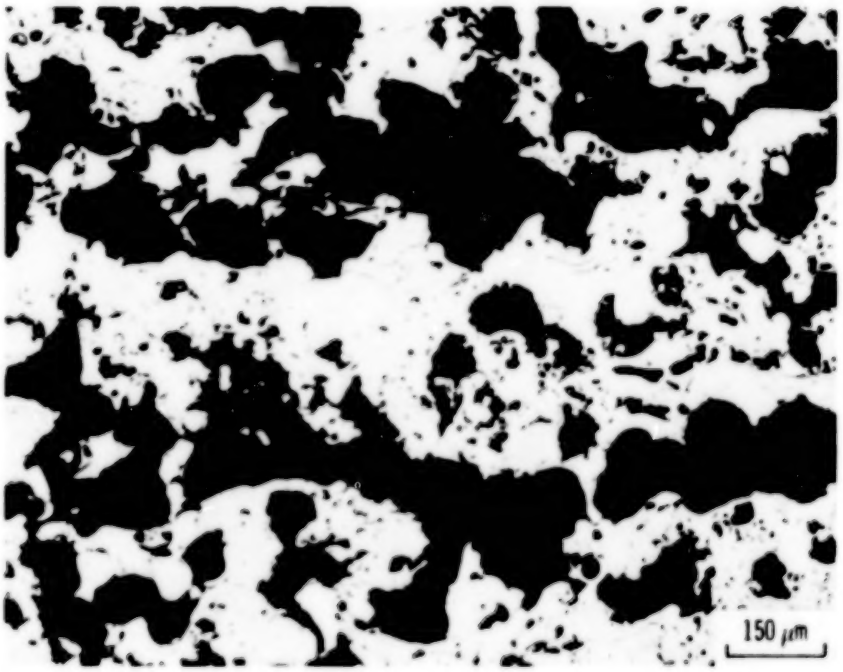

(b) Polyester spray parameters.

Figure 15. - Microstructures of plasma-sprayed NiCrAlY-polyester powder mixtures resulting from use of NiCrAlY and polyester plasma-spray parameters. NiCrAlY spray parameters were used in preparation of thermal shock specimens.

thermal shock cycles. Note spongy, porous structure.

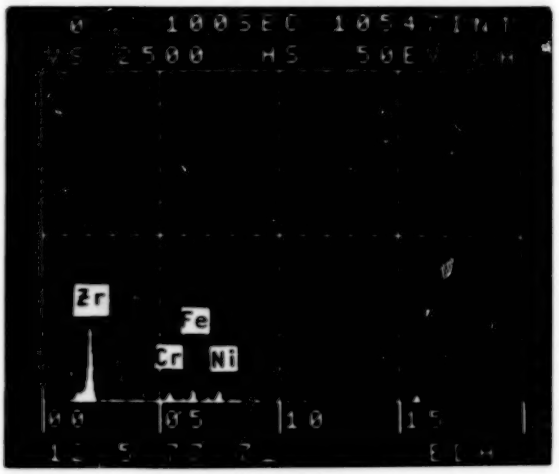

(b) Elemental analysis of ceramic, showing presence of nickel, iron, and chromium from bond coat and substrate. Aluminum peak coincides with zirconium peak.

Figure 16. - NiCrAlY-YSZ interface in LM-1 specimen after 455 thermal shock cycles.

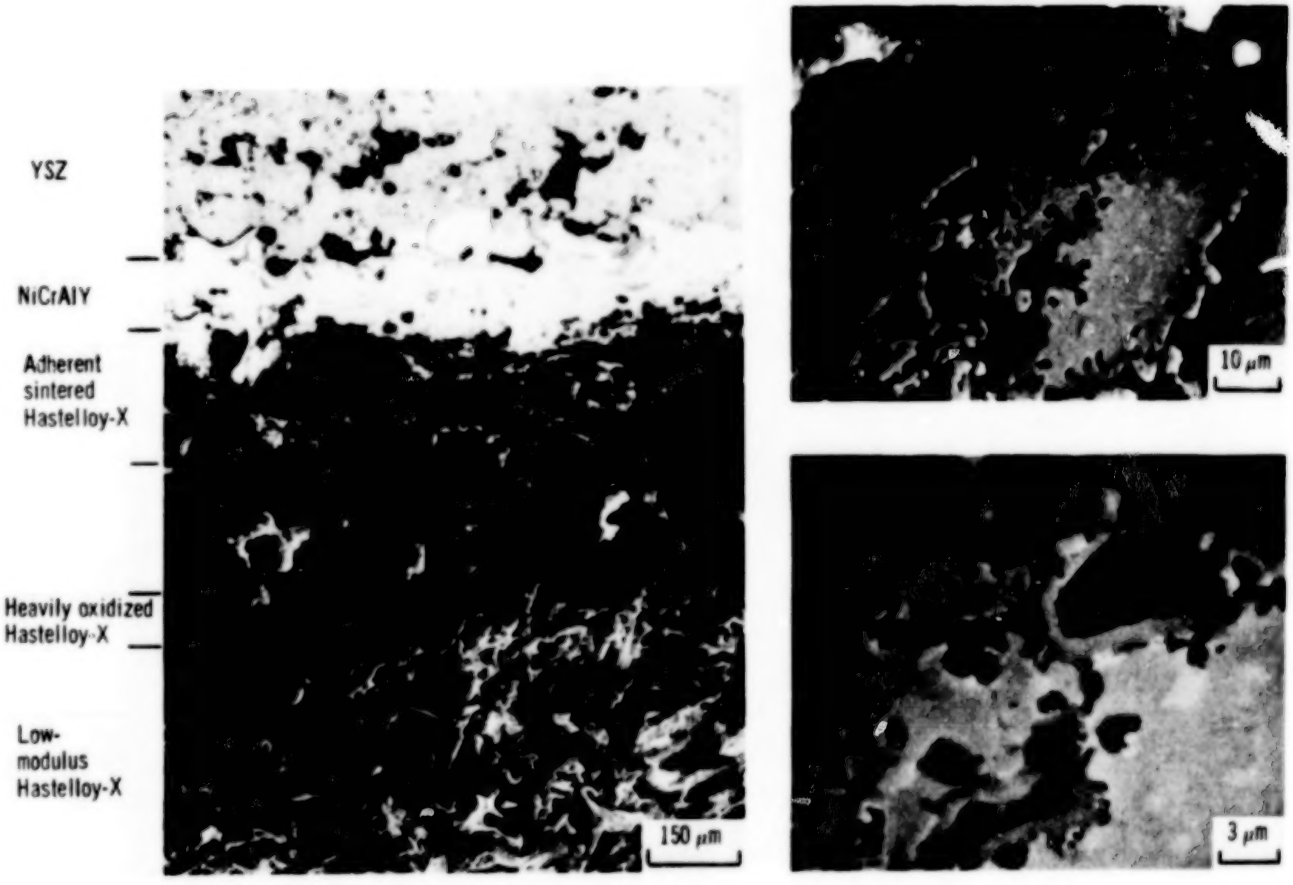

Figure 17. - Microsection through laminar crack in system LM-2, showing evidence of heavy oxidative damage to sintered, low-density Hastelloy-X pad.

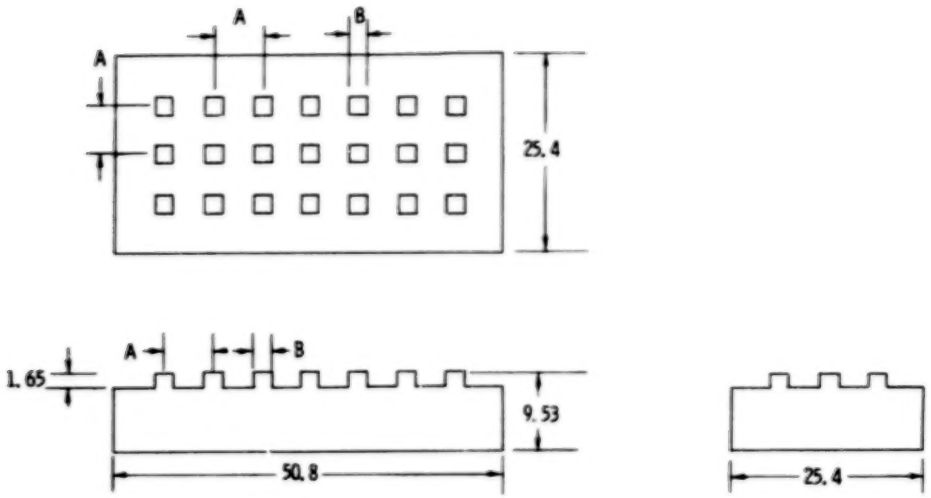

Cooling-pin array	Pin spacing, A, mm	Pin thickness, B, mm
I	3.18	1.14
II	3.18	.635
III	6.36	1.14

Figure 18. - Schematic of cooling-pin arrays machined on 304-stainless-steel backings. (Dimensions are in millimeters.)

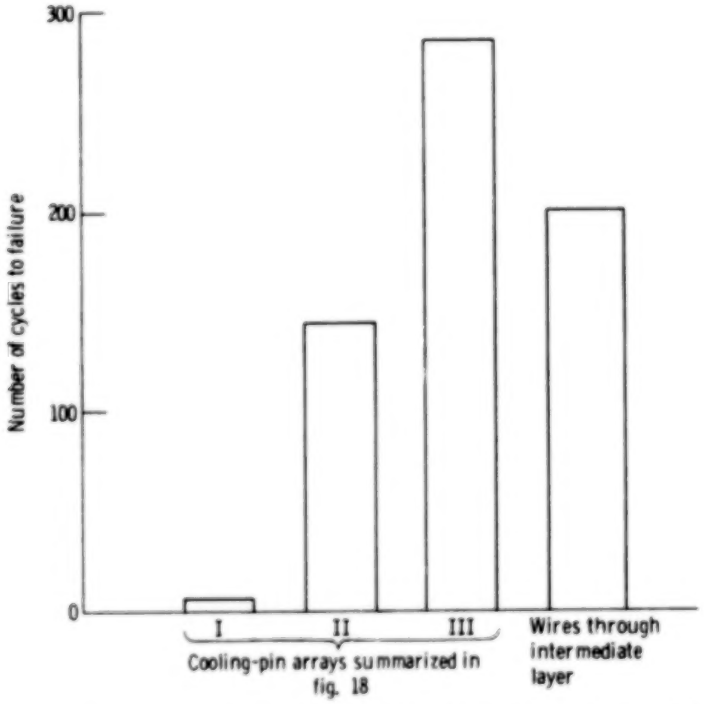

Figure 19. - Cyclic thermal shock lives of low-modulus-pad intermediate layer specimens incorporating various cooling-pin arrangements. (LM-3 low-modulus material used.)

1. Report No. NASA TP-1561 AVRADCOM TR 79-28	2. Government Accession No.	3. Recipient's Catalog No.
4. Title and Subtitle PRELIMINARY STUDY OF METHODS FOR PROVIDING THERMAL SHOCK RESISTANCE TO PLASMA-SPRAYED CERAMIC GAS-PATH SEALS		5. Report Date May 1980 6. Performing Organization Code
7. Author(s) Robert C. Bill, Donald W. Wisander, and David E. Brewe		8. Performing Organization Report No. E-9941 10. Work Unit No. 505-04
9. Performing Organization Name and Address Propulsion Laboratory, AVRADCOM Research and Technology Laboratories, Lewis Research Center, Cleveland, Ohio and NASA Lewis Research Center, Cleveland, OHio 44135		11. Contract or Grant No.
12. Sponsoring Agency Name and Address National Aeronautics and Space Administration Washington, DC 20546 and U.S. Army Aviation Research and Development Command St. Louis, MO 63166		13. Type of Report and Period Covered Technical Paper 14. Sponsoring Agency Code

15. Supplementary Notes
Robert C. Bill, AVRADCOM Research and Technology Laboratories; Donald W. Wisander, Lewis Research Center; David E. Brewe, AVRADCOM Research and Technology Laboratories.

16. Abstract
The cyclic thermal shock resistance of several outer air, gas-path seal systems for high-pressure turbines was evaluated. In all these systems, plasma-sprayed, yttria-stabilized ZrO_2 was the ceramic constituent. The most promising approaches were those that had a porous-metal, low-modulus pad as a strain isolator between the ceramic layer and the dense metal substrate. Cooling pins extending into the low-modulus pad significantly reduced the oxidation rate of the porous metal and the extended seal life. The thermal shock resistance of the ceramic layer was improved by increasing its porosity and by precracking it before thermal shock testing. Microstructural and probe studies suggested that the long-term durability of the high-pressure-turbine seal systems would be adversely affected if the metal-ceramic interfaces exceeded about 800° C because some metallic species would rapidly diffuse.

17. Key Words (Suggested by Author(s))
Abradable seal
Ceramic
Zirconium oxide
Thermal shock
Plasma spray

18. Distribution Statement
Unclassified - unlimited
STAR Category 27

19. Security Classif. (of this report)	20. Security Classif. (of this page)	21. No. of Pages	22. Price*
Unclassified	Unclassified	23	A02

* For sale by the National Technical Information Service, Springfield, Virginia 22161

NASA-Langley, 1980